

RESEARCH ARTICLE

Pendulum-based measurements reveal impact dynamics at the scale of a trap-jaw ant

Justin F. Jorge^{1,*}, Sarah Bergbreiter² and S. N. Patek¹

ABSTRACT

Small organisms can produce powerful, sub-millisecond impacts by moving tiny structures at high accelerations. We developed and validated a pendulum device to measure the impact energetics of microgram-sized trap-jaw ant mandibles accelerated against targets at 10^5 m s^{-2} . Trap-jaw ants (*Odontomachus brunneus*; 19 individuals, 212 strikes) were suspended on one pendulum and struck swappable targets that were either attached to an opposing pendulum or fixed in place. Mean post-impact kinetic energy (energy from a strike converted to pendulum motion) was higher with a stiff target (21.0–21.5 μJ) than with a compliant target (6.4–6.5 μJ). Target mobility had relatively little influence on energy transfer. Mean contact duration of strikes against stiff targets was shorter (3.9–4.5 ms) than against compliant targets (6.2–7.9 ms). Shorter contact duration was correlated with higher post-impact kinetic energy. These findings contextualize and provide an energetic explanation for the diverse, natural uses of trap-jaw ant strikes such as impaling prey, launching away threats and performing mandible-powered jumps. The strong effect of target material on energetic exchange suggests material interactions as an avenue for tuning performance of small, high acceleration impacts. Our device offers a foundation for novel research into the ecomechanics and evolution of tiny biological impacts and their application in synthetic systems.

KEY WORDS: Elastic systems, Latch-mediated spring actuation, *Odontomachus*, Ecomechanics, Energy measurement

INTRODUCTION

Many organisms generate extreme, transient impacts through the acceleration of lightweight structures. Mantis shrimp fracture shells by accelerating small appendages up to 10^5 m s^{-2} (McHenry et al., 2016). Panamanian termites strike nest invaders with 0.03 mg mandibles accelerated up to 10^6 m s^{-2} (Seid et al., 2008). Other arthropods, such as trap-jaw spiders and trap-jaw ants, strike prey with ultrafast mandibles (Larabee and Suarez, 2014; Wood et al., 2016). To understand the mechanics and energetic consequences of this strategy of coupling small mass with high acceleration, it is essential to measure impact energetics at the temporal and spatial scales of these organisms and across their rich array of target materials and dynamics. With recent discoveries establishing the differential scaling of material dynamics at small sizes and under rapid deformation (Anderson, 2018; Anderson et al., 2016;

Ilton et al., 2018, 2019), testing the impact dynamics at the temporal and spatial scale of the organism's use of the mechanism is likely to reveal new insights about the impact dynamics of these systems that are obscured through traditional scaled impact tests that only match energetic inputs. Here, we analyzed the impact energetics of trap-jaw ants toward the goal of establishing foundational approaches and questions related to measuring high acceleration impacts at small scales.

Trap-jaw ants use the potent impacts of their extremely fast mandible strikes in a range of contexts. In a tenth of a millisecond, they accelerate their mandibles up to 10^5 m s^{-2} , with a mass-specific power output of 100 kW kg^{-1} (Larabee et al., 2017; Patek et al., 2006; Spagna et al., 2008). Depending on their target's material and mass, trap-jaw strikes ensnare or puncture the target, propel the target away, launch their own body into the air, or propel both themselves and their target away from the site of impact (Spagna et al., 2009). They use these impacts to capture prey, defend against threats and perform mandible-powered jumps by directing strikes against the ground (Carlin and Gladstein, 1989; Patek et al., 2006; Spagna et al., 2009). In addition to jumping with their mandible strikes from leaf litter and solid ground, they also launch themselves off of sand in antlion pit traps (Larabee and Suarez, 2015). In sum, trap-jaw strikes apply intense, transient impacts against a wide range of biological (e.g. 10^{-2} GPa larval to 10^2 GPa adult insect cuticle; Vincent and Wegst, 2004) and inorganic materials (e.g. rocks, sand and soil; Fig. 1; see Aguilar and Goldman, 2016; Huang et al., 2020; Umbanhowar and Goldman, 2010 for nonlinearity of substrate behavior). However, the impact energetics of trap-jaw ant mandible strikes and other small, high-acceleration impacts have rarely been measured experimentally.

Direct measurements of impacts at the scale of trap-jaw ants push the limits of technology. Impacts are traditionally measured via high-speed imaging, accelerometers and force sensors. However, these tests are designed for systems at larger spatial and temporal scales than ant strikes. Trap-jaw ant strikes occur at sub-millisecond scales with millimeter-long, $50 \mu\text{g}$ mandibles (Gibson et al., 2018; Patek et al., 2006; Spagna et al., 2008, 2009). Limited temporal resolution of high-speed imaging rules out filming impacts: trap-jaw ant impacts occur within a single frame of a $300,000 \text{ frames s}^{-1}$ image sequence. Accelerometers (which must be attached to the mandibles) would interfere with strike dynamics, because small commercially available accelerometers are typically in the milligram scale, which means that they are more than 100 times the mass of a mandible (micrograms). Custom-built microdevices for comparative biomechanics are similarly constrained, and are often wired, adding additional mass (Byrnes et al., 2008; Spence et al., 2010). Even piezoelectric load cells that are designed for measuring transient impacts are problematic at these scales. A sensor would need to have a natural frequency of 600 kHz or a period of 0.0017 ms to accurately record impact. Piezoelectric impact sensors typically have a natural frequency of 75 kHz with a period of 0.013 ms and thus cannot

¹Biology Department, Duke University, Durham, NC 27708, USA. ²Department of Mechanical Engineering, Carnegie Mellon University, Pittsburgh, PA 15213, USA.

*Author for correspondence (jff7@duke.edu)


 J.F.J., 0000-0002-7030-0610; S.B., 0000-0003-2735-0206; S.N.P., 0000-0001-9738-882X



Fig. 1. Trap-jaw ants live in environments composed of diverse substrates. In addition to using their mandibles to interact with diverse biotic targets such as prey or threats, these ants can perform mandible-powered jumps by slamming their mandibles into the substrate. Standing outside of a trap-jaw nest at the Archbold Field Station in Florida, the ant in the center has its mandibles in the open position and is ready to strike (photo by J.F.J.).

resolve transient impacts by small organisms. Piezoelectric film tests have been applied to trap-jaw ants; however, this method requires rigorous calibration such that visualization of impacts throughout the depth of the film can be analyzed appropriately (Hao et al., 2018). Small mandibles moving at high accelerations thus limit the application of traditional approaches.

Drop towers and pendulum-based materials tests are used at larger scales to characterize the energetic exchange of transient, high-speed impacts. For example, Charpy and Izod tests report the energetics of material failure by measuring the deceleration of a pendulum as it swings through a sample (ASTM International, 2018a,b). Drop towers measure the rebound of a mass after it impacts a sample. From this, a coefficient of restitution can be calculated to represent the change in velocity of the dropped mass before and after impact. These approaches have been applied to biological systems through an energetic scaling approach whereby the mass is increased and velocity decreased such that they match the energetics of the organism's impact. For example, ball-drop tests and coefficient of restitution calculations have revealed the effectiveness of mantis shrimp telson armor for dissipating the energy from conspecific strikes (Taylor and Patek, 2010), and high-speed puncture tests investigated the dynamics of target materials (Anderson et al., 2016). Likewise, a pendulum-based approach established the energy absorbed by the cockroach exoskeleton during impact-mediated transitions from running to climbing (Jayaram et al., 2018).

These approaches and other similar experiments (Lee et al., 2011; Swift et al., 2016) match the energetic input during scaled impact tests, yet they rely on the assumption that material dynamics and losses scale isometrically across both temporal and spatial scales. These assumptions are valid for larger systems; however, recent studies have demonstrated that, at the spatial and temporal scales of ultrafast organisms and transient impacts, the dynamics of materials do not scale isometrically (Ilton et al., 2018, 2019). Specifically, the inertia of materials is disproportionately important at the small spatial and temporal scales of these organisms, thereby causing a substantial shift in their dynamics. Therefore, the dynamics of impacts at these scales is also likely to diverge from the scaled-up models of traditional impact tests that only match energetics of momentum or kinetic energy of the incoming projectile. Finally, small organisms

using repeated impacts must withstand repeated use; therefore, these systems should operate in the inelastic region to repeatedly absorb or dissipate impact energy, and avoid failure (Biewener and Patek, 2018). In sum, the central goal of the present study was to develop, test and apply an approach to measuring impact dynamics at the exceedingly challenging, *in vivo*, temporal and spatial scales of small, ultrafast organisms that does not rely on the materials and loss assumptions of traditional scaled drop tests.

We examine the impact energetics of trap-jaw ant strikes by developing and validating a novel, modular pendulum impact tester and then applying it to address foundational questions about the energetic exchange of trap-jaw strikes across varying targets. The new pendulum device measures both the response of swappable targets to impacts from small organisms as well as the response of the organisms themselves, with the organism's impact energy serving as the energy source. As discussed above, even though the physics of impact mechanics and energetic exchange are thought to scale across systems, few, if any, studies have examined the energetics of impacts at the size, duration and acceleration of small organisms, such as the trap-jaw ant. Consequently, given current understanding, it is equally possible that trap-jaw ant impacts: (1) exhibit equivalent energetic exchange to standard materials drop tests if the physics of material exchange scale similarly; (2) exhibit lower energetic exchange (i.e. more damping and loss) given the small scales and the dominance of friction and viscosity at these scales; and (3) exhibit greater energetic exchange given the short duration of impact and the insufficient time for viscoelastic energy losses to accumulate. The outcome of these tests enables and guides future ecomechanics research that can be scaled up to more feasible spatial and temporal scales such that standard impact testing tools can be employed, or the findings may indicate the need to use live animals and their naturalistic targets to properly inform the energetic exchange across diverse mechanisms, impacts, accelerations and habitats of these organisms. We began with the most basic question: how is kinetic energy from impact distributed between the impactor and target, and can a pendulum device accurately and consistently report impact energetics? Given that our pendulum impact tester successfully measured impact energetics at this scale, we then asked: what are the effects of target material and target movability on the energy delivered to the target during impact? Finally, we asked how contact duration during impact influences energetic exchange between source and target. In the process of answering these questions, we validated that this pendulum impact tester can successfully resolve energetic exchange at small scales and we informed a foundational experimental paradigm and measurement approach to small-scale impacts in biology.

MATERIALS AND METHODS

Pendulum design

We developed the micro impact characterization pendulum (mICP) to convert the energy from small-scale, transient impacts against a target into measurable kinetic energy represented by pendulum motion. The mICP consisted of an energy source and a target with one or both suspended from an impact response pendulum, which consisted of a 3 mm diameter, 90 mm long carbon fiber tube with an air bearing (13 mm inner diameter Roller Air Bearing, OAV, Princeton, NJ, USA) as a near-frictionless point of rotation (Fig. 2B). Unlike ball bearings, air bearings use a thin layer of air rather than small spheres to separate the inner race from the outer race. This primarily prevented energy loss due to heat from components sliding across each other and also allowed for increased consistency between uses as there was negligible wear on the air bearing components.

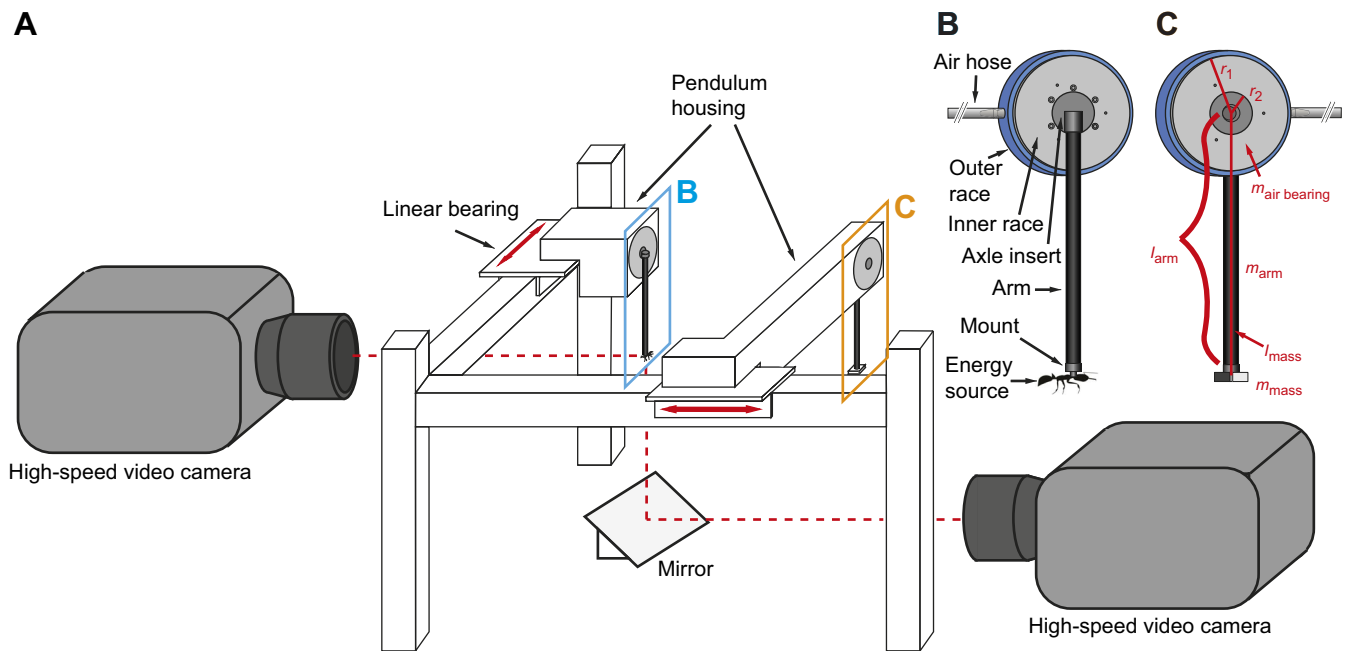


Fig. 2. The micro impact characterization pendulum (mICP) uses two pendulums to measure the post-impact kinetic energy from both the trap-jaw ant and its target. (A) The mICP is composed of a dual pendulum mounting system that is filmed from the side and from below. Motion in both pendulums caused by impact from the energy source is recorded by two high-speed video cameras. Mounting the pendulum housings on linear bearings enables fine adjustment of the pendulums along a rail system, keeping experiments consistent across trials. (B) The impactor pendulum can be lifted to specific heights during the validation phase or instrumented with an impacting animal as the energy source during the testing phase. A custom-built mount inserts into the end of the pendulum arm and attaches the energy source, which is either a live trap-jaw ant (shown here) or a validation impactor outfitted with trap-jaw ant mandibles to match the impacting surface and materials of the live animals. (C) The target pendulum recreates the impactor assembly with a target replacing the energy source. For both pendulums (B,C), an air bearing is used as the point of rotation. The inner race of the air bearing rotates while the outer race is held in place by the pendulum housing. To decrease friction between the outer race and inner race, air is forced into the bearing from the compressed air source (not depicted). A custom-built axle insert allows the pendulum arm, a 3 mm diameter carbon fiber tube, to be attached to the rotating inner race. In red are the measurements used for calculation of the rotational kinetic energy of the pendulum. Note that for impacts against a fixed target, the target pendulum (C) is pushed aside and replaced with a fixed form of the target (see Fig. 3 for details).

For our study, a trap-jaw ant was the energy source. The ant was attached to the impact response pendulum at the point where the head joins the pronotum to limit energy dissipated by head recoil after a strike. The ant then impacted a target that was either fixed in place or suspended on its own impact response pendulum (Movie 1), which resulted in either the target not moving (fixed condition) or the target swinging backwards on its pendulum away from the location of impact. When the target was fixed in place, energy from the impact was measured as the rotational kinetic energy of the pendulum from which the organism was suspended. Rotational kinetic energy ($E_{K,rot}$) was calculated using the following equation:

$$E_{K,rot} = \frac{1}{2} I \omega^2, \quad (1)$$

where I is defined as the moment of inertia of the entire pendulum assembly and ω refers to the angular velocity of the pendulum. To simplify the calculation of the moment of inertia, the study organism was approximated as a point mass (m_{mass}) at a distance l_{mass} from the point of rotation. The hollow carbon fiber tube that constitutes the pendulum arm was modeled as a hollow cylinder with an inner radius r_{a1} , an outer radius r_{a2} , a length l_{arm} and a mass m_{arm} located $l_{arm}/2$ away from the point of rotation. Finally, the portion of the air bearing that rotates must also be included in the equation for inertia. We modeled the air bearing as a thick-walled cylinder rotating about its central axis. This cylinder has a mass $m_{air bearing}$, a radius from the center axis to the outer race of the cylinder r_{b1} , and a radius from the center axis to the inner race of the cylinder r_{b2} (Fig. 2C). Adding

these inertia calculations together yielded the equation:

$$I = \frac{1}{3} m_{arm} l_{arm}^2 + m_{arm} \left(\frac{r_{a1}^2 + r_{a2}^2}{4} \right) + m_{mass} l_{mass}^2 + \frac{1}{2} m_{air bearing} (r_{b1}^2 + r_{b2}^2). \quad (2)$$

Angular velocity, ω , was calculated by dividing the change in angular displacement over time:

$$\omega = \frac{\Delta\theta}{t}. \quad (3)$$

For the energy calculations, we used the average angular velocity sampled over the first 5 ms after impact. By sampling immediately after impact, the accumulated energetic losses due to drag were reduced. Angular displacement, $\Delta\theta$, was calculated through a rearrangement of the equation for the law of cosines, for which x was the distance traveled by the pendulum during a set amount of time and l was the length of the pendulum:

$$\theta = \cos^{-1} \left(\frac{2l^2 - x^2}{2l^2} \right). \quad (4)$$

To calculate the change in the position of the pendulum over time, we filmed the strikes against the targets at 3000 frames s^{-1} with a high-speed video camera (1024×1024 pixel resolution, 1/3015 s shutter duration; SA-X2, Photron, San Diego, CA, USA). We digitized the high-speed videos using an automated routine that

converted the position of the study system over time into its x and y components (DLTdv6 MATLAB script; MATLAB 9.4, version R2018a; Hedrick, 2008).

For impacts against targets that were also suspended on a pendulum, energy from impact was measured as the sum of kinetic energy from both the motion of the target pendulum and the motion of the pendulum from which the study system is suspended. Rotational kinetic energy from the target pendulum was calculated using the previously mentioned equations, in which the mass of the target was simplified as a point mass. Pendulum design, material selection and experimental conditions are revisited in detail in the Discussion.

Pendulum verification and material testing

Our experiments tested impacts against two target materials under two conditions: (1) target fixed in place, and (2) target attached to an impact response pendulum, allowing the target to swing freely after an impact (Fig. 3B). These target types (stiff and compliant material under the two conditions) are the same as those later tested against the trap-jaw ant strikes. Before running our experiments with a live

trap-jaw ant as the energy source, we ran a series of tests to validate the device and assess the variability of the energetic output. This approach ensured that the impact response pendulum accurately detected the effects of the different target types. Each target type was tested multiple times while using a controlled energy input and a consistent impactor surface. Specifically, we attached a validation impactor to the impact response pendulum instead of a trap-jaw ant to form an impactor pendulum. The validation impactor was constructed to match a trap-jaw ant's impact surface and body mass by attaching trap-jaw ant mandibles with cyanoacrylate glue to a cuboid that was within the mass of a trap-jaw ant (6 mg; $0.75 \times 1.5 \times 4.0$ mm cuboid; 3D printed, Grey Pro Resin, Form 2, Formlabs, Somerville, MA, USA). We raised the impactor pendulum to starting heights with potential energies that were within the expected range of trap-jaw strike energy outputs (Movie 2). This test was conducted at 15 different input energies against each target type (Fig. 3 and next section).

We filmed the pendulum tests with a high-speed camera (3000 frames s^{-1} , 1024×1024 pixel resolution, $1/3015$ s shutter duration; SA-X2, Photron) and measured input energy by calculating the kinetic energy of the impactor immediately before contact with

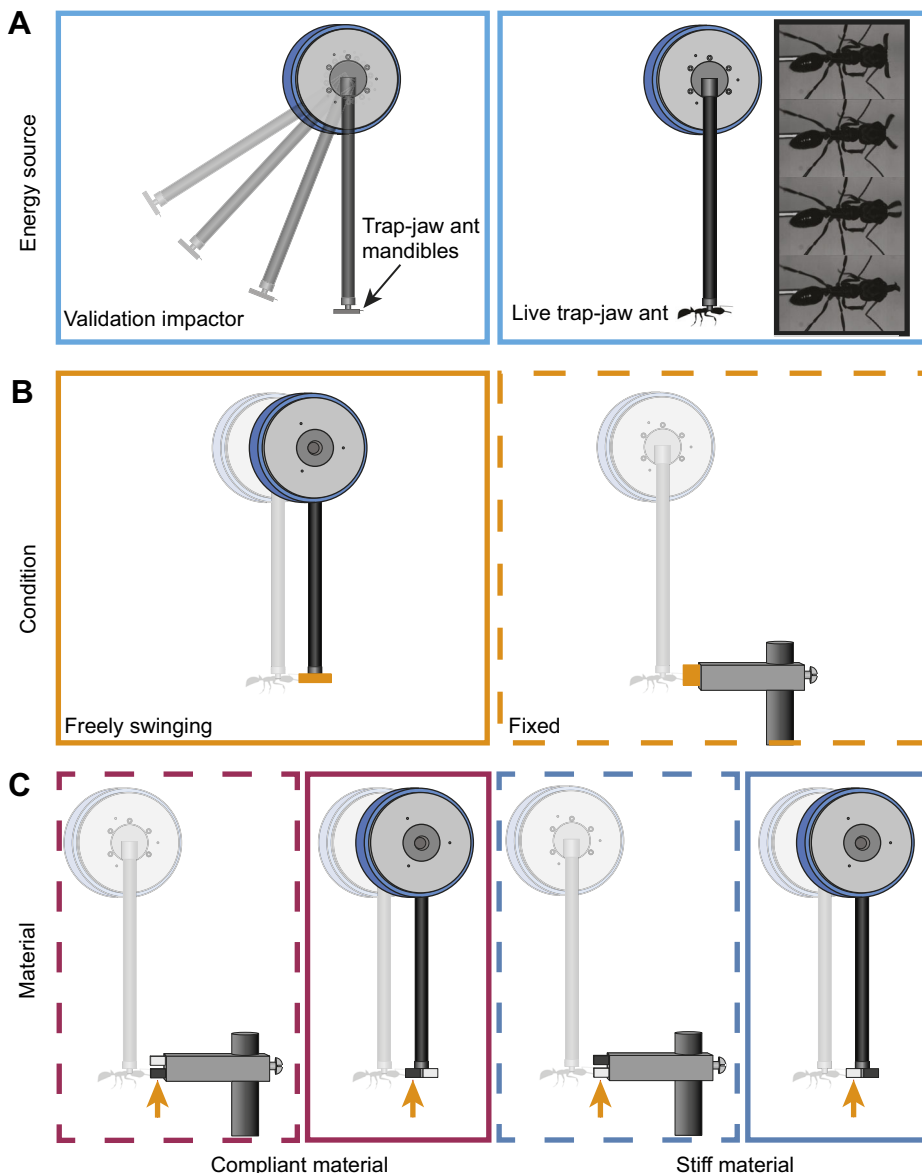


Fig. 3. The mICP is validated via controlled impactor tests and then used for trap-jaw ant impact experimental tests. (A) The energy source is either a validation impactor with ant mandibles glued to its surface and lifted to set heights with known input energy (left) or a pendulum with a live trap-jaw ant impacting its target (right). The image sequence (inset) depicts a trap-jaw ant strike filmed at 210,000 frames s^{-1} with 5 frames (0.023 ms) separating each image. (B) In each test, the target pendulum is either freely swinging (left) or fixed in place (right). (C) We tested two target materials under the fixed (dashed outline) or freely swinging (solid outline) conditions. Sorbothane is the more compliant target material (left, maroon outline). Spring steel is the stiff target material (right, blue outline). In order to test the two different materials while keeping mass constant, the target can be flipped (yellow arrow). The energy source in B and C is depicted as a live trap-jaw ant, but note that we also performed the controlled validation tests (A, left) against these same target configurations (C).

the target. Post-impact kinetic energy was measured by calculating the kinetic energy of the impactor pendulum immediately after contact. When the target was suspended on a pendulum, the target's kinetic energy was also calculated and included in the post-impact kinetic energy calculation.

Statistical analyses were conducted on the ratio of input energy to post-impact kinetic energy, which we henceforth term the kinetic energy (KE) ratio, to determine the ability of the pendulum setup to distinguish impact dynamics across the different target types. The KE ratio represents the proportion of initial energy remaining as pendulum motion after the impact. An ANOVA test was conducted as well as multiple Welch two-sample *t*-tests comparing the means of all target KE ratios to each other (v.3.6.1; R Foundation for Statistical Computing, <https://www.r-project.org/>). All analyses and R code are archived in Dryad (<https://doi.org/10.5061/dryad.b2rnbzsbm>; Jorge et al., 2021).

Additional statistical analyses were performed on the standard deviation of the KE ratio to determine the precision of the device and variation across target types. We modified the ASTM standard for repeatability outlined in ASTM standard E691 (ASTM International, 2019a) to measure precision across trials for each target type. This standard uses an *F*-test to evaluate whether a method yields consistent results across different laboratories running the same test under similar conditions (ASTM International, 2019a). As this is not an interlaboratory test, we instead used the test to determine whether the pendulum behaved similarly across target types, measured by the KE ratio. This test compared each target's repeatability (*k*). We define *k* using the standard deviation of the KE ratios from the 15 impacts within an individual target test, *s*, divided by the average variability across all target tests, *s_r*, which was calculated with the following equation:

$$s_r = \sqrt{\frac{\sum_{i=1}^n s_i^2}{n}}, \quad (5)$$

where *n* is the number of target groups (in this case, 4). A *k*-value greater than 1 indicated that the KE ratio standard deviation was higher within the individual target's tests than the average standard deviation of all target tests. *k_{critical}* was then used to determine whether one target's KE ratio standard deviation was significantly higher than another. Each *k* value was compared with *k_{critical}*, determined by the equation:

$$k_{\text{critical}} = \sqrt{\frac{n}{1 + \frac{n-1}{F}}}, \quad (6)$$

where *F* represents the *F*-value evaluated at the 0.5% significance level (alpha of 0.005) with 14 and 42 degrees of freedom, respectively. Impacts with *k*-values higher than *k_{critical}* were determined to have KE ratio standard deviations significantly larger than the rest of the targets.

Measuring impact dynamics of trap-jaw ants

We applied the mICP to measure impact dynamics of mandible strikes from the trap-jaw ant *Odontomachus brunneus* (Patton 1894) (referred to throughout this paper as trap-jaw ant). Nineteen workers (average mass of 7 mg) were picked at random from a queenright colony for these experiments. The colony was collected from the Archbold Field Station in Florida (permit P526P-19-02953) and kept in an artificial nest consisting of two Petri dishes with dental plaster as their substrate joined together with rubber tubing. Dental

plaster holds water when wetted and served as a source of water for the ants. The colony was fed a mealworm every 2 days and had access to sugar water *ad libitum* to fulfill their dietary needs.

Trap-jaw ants perform rapid strikes with 1 mm long mandibles (Fig. 3A) and readily strike against a wide range of targets. We induced strikes by slowly moving targets within range of the trigger hairs that extend from the base of the mandibles. The target was brought towards the ants so slowly that we could assume that the strikes occurred under quasistatic conditions. Prior to a strike, the mandibles rotate laterally such that they are perpendicular to the sides of the head and are then locked in place (Gronenberg, 1995). In this locked position, adductor muscles contract to store energy in elastic elements including the apodeme and head capsule (G. P. Sutton, R. St. Pierre, A., Guo, C.-Y. Kuo and S.N.P., unpublished results). When provoked, trap-jaw ants, aided by their trigger hairs (Gronenberg and Tautz, 1994), position their mandibles close to the target and release the latching mechanism.

Like most biological movements, trap-jaw ant impacts are not 'typical' pendulum impacts, such as those in the impactor experiments described above. Therefore, additional parameters were needed to assess their impact energetics. For example, trap-jaw ants rotate their mandibles toward the target, such that the mandible tips might briefly drag against the target during impact. Furthermore, the distance between the mandibles and the target prior to the strike could influence where the impact occurs along the mandible's arc-like path. Therefore, we added an additional high-speed camera to film the mandible motion during impact. This high-speed camera (210,000 or 300,000 frames s⁻¹, 256×128 pixel resolution, 2.33 μs shutter speed; SA-Z, Photron) was aimed at a mirror tilted at 45 deg below the pendulums to capture a ventral view. With these videos, we measured the distance between the mandibles and target prior to impact and the contact duration of the mandibles during impact. Our ability to hold the distance relatively constant prevented variation in distance across target groups. We conducted a Mann–Whitney *U*-test to determine whether distances for strikes against the stiff target and strikes against the compliant target were significantly different. Similarly, to determine the effects of target type on contact duration, we ran a series of Mann–Whitney *U*-tests.

As a test of the effects of materials on impact energetics, the trap-jaw ants struck targets made of two different materials that were either fixed in place or free to swing on their own pendulum (Fig. 3B). One material was a viscoelastic polyurethane material used commercially to dampen vibrations (bulk modulus=5 GPa; 4000 Durometer Sorbothane, Sorbothane, Kent, OH, USA). It was referred to as the compliant material because it was the least stiff of the two. Spring steel was used as the stiffer material (bulk modulus=140 GPa; 1095 Spring Steel Machine Key Stock 98535A150, McMaster-Carr, Elmhurst, IL, USA). Damping was also relatively higher in the compliant material when compared with the stiff material given its intended use in vibration isolation (the tanΔ at 50 Hz for 4000 Sorbothane is 0.65 to 0.8). To test the two materials while controlling for target mass, we created a target with two halves, each 6×3×2 mm and made from a different material. The Sorbothane and spring steel halves were attached to either side of a 1 mm thick mount that was then press-fit onto the end of the impact response pendulum arm, resulting in a completed target 7×6×2 mm in size with a mass of 0.4 g regardless of the test material being used in a particular experiment (Fig. 3B).

When measuring strikes against a fixed target, only the ant was suspended from an impact response pendulum. To create the target for these experiments, the test materials were fashioned into blocks with the same dimensions (6×3×2 mm) as the two halves that

constituted the target in the aforementioned two-pendulum setup, but were instead attached above and below each other on the face of a metal plate (Fig. 3C). A hole through the metal plate allowed it to move vertically along a metal post and a set screw secured it onto the post at the desired height. The metal post was fastened to a linear translation stage micromanipulator (XR25C, Thorlabs, Newton, NJ, USA) for precise positioning of the target.

Our experiments consisted of each ant performing three strikes on each of the four target types (a freely swinging compliant target made of Sorbothane, a freely swinging stiff target made of spring steel, a fixed compliant target made of Sorbothane, and a fixed stiff target made of spring steel) for a total number of 12 strikes per ant. The order of the tests (e.g. whether the ant first struck a fixed stiff target, a freely swinging compliant target, etc.) was generated randomly (Random.org). However, some ants would stop striking before completing all four target types, which resulted in fewer strikes for the individual. Ants that completed the 12 strikes were allowed to keep striking the target types in the reverse order of the randomly generated sequence (maximum of 24 strikes allowed). In total, we collected a total of 212 mandible strikes from 19 ants (3 to 23 strikes per individual).

The KE ratio used in the previous section to validate the device was not applicable to the tests with a live trap-jaw ant energy source. The KE ratio requires an accurate measurement of the amount of initial energy. However, accurately measuring input energy from the trap-jaw ant would have required the ability to calculate the amount of energy from the closing of the mandibles (see Appendix). Instead, statistical analysis of trap-jaw ant performance across the four target types focused on the amount of post-impact kinetic energy. Owing to differences in sample sizes for each target type, we conducted a series of Mann–Whitney *U*-tests between the different target types to determine whether there were any significant differences between energy measurements (R v.3.6.1).

Using statistical models, we assessed how these parameters affected the amount of energy transferred during a strike. We compared linear and multi-level models using Bayesian statistics and WAIC (widely applicable information criterion, Rethinking package; McElreath, 2016; R v.3.6.1). Parameters included target materials impacted by the ant, whether the target was fixed or unfixed, contact duration, distance between the ant and the target, individual ant ID, and strike order (i.e. how far along the ant was along the series of strikes). The code for each model is available from Dryad (<https://doi.org/10.5061/dryad.b2rbnzsmb>; Jorge et al., 2021).

RESULTS

Pendulum and material characterization

The mICP distinguished differences in impact energetics across the four targets. By comparing the ratio of the amount of energy in the motion of the pendulums after the strike to the amount of initial energy (KE ratio) for the target types, we found that impact dynamics varied across the four target types (Fig. 4). Higher KE ratios indicate that more of the initial energy was converted into pendulum motion after the impact. Our tests determined the following ranking of targets from highest KE ratio to lowest KE ratio: freely swinging stiff, fixed stiff, freely swinging compliant and fixed compliant (Table 1). The KE ratios were significantly different across all target types (ANOVA, d.f.=3,56, $F=186$, $P<0.001$, all Welch two-sample *t*-tests $P<0.0015$).

We tested the consistency of the device by comparing the standard deviation of the KE ratio within a target type and across target types (Table 1). The KE ratio standard deviation for each target type supported consistent pendulum performance across the

15 impacts of various initial energies. Standard deviation was higher in stiff targets compared with compliant targets. Standard deviations of fixed stiff targets were significantly different, whereas standard deviations of the other target types were not significantly different (Table 1). Fixed stiff targets exhibited the highest variation ($k=1.41$ compared with $k_{\text{critical}}=1.39$).

Measuring impact dynamics of trap-jaw ants

Fixing the target in place did not significantly affect energy transfer, whereas target stiffness did (Table 2). Post-impact kinetic energy for strikes against fixed compliant targets was not significantly different than for strikes against freely swinging compliant targets. Likewise, post-impact kinetic energy values of fixed stiff targets and freely swinging stiff targets were not significantly different. However, strikes against compliant targets had significantly lower post-impact kinetic energy than strikes against stiff targets (Fig. 5A, statistical summary in Table 3). For strikes against a compliant target that was free to swing on a pendulum, more energy was transferred back into the ant pendulum than into the target pendulum (average of 1.65 times more energy for strikes against free, compliant targets, average of 1.53 times more energy for strikes against free, stiff targets; Fig. 5B).

The distance between the ant and target was distributed around 0.50 mm (Fig. 6). The median distance between the ant and the compliant target (including both conditions) was 0.43 mm, whereas the median distance for the stiff target was 0.47 mm. The difference between these two medians was not significant (Mann–Whitney $U=4803.5$, $n_1=105$, $n_2=107$, $P=0.06$, two-tailed).

Contact duration

Contact duration was a key influence on impact energetics. Strikes against the targets exhibited three phases: (1) initial impact and bouncing of the mandibles against the surface; (2) continuous contact with the surface and the sliding of the mandibles across the target's surface; and (3) separation (Movie 3). These phases were observed in strikes across all four target types. Phase 1 is used for defining impact duration, which is the duration of the initial mandible contact with the target. Contact duration encompasses phases 1–3, and is defined as the duration from initial target contact to the final separation of the mandibles from the target.

Contact duration varied by target material. In general, strikes against the stiff targets had a shorter contact duration than those against a compliant target (Table 2, Fig. 7). Strikes against fixed, compliant targets had significantly increased contact durations when compared to freely swinging, compliant targets (medians of 7.4 ms versus 6.1 ms; Mann–Whitney $U=2030$, $n_1=50$, $n_2=55$, $P<0.001$, two-tailed). Similarly, strikes against fixed, stiff targets had significantly increased contact durations when compared to freely swinging, stiff targets (4.5 ms versus 3.7 ms; Mann–Whitney $U=2082$, $n_1=52$, $n_2=55$, $P<0.001$, two-tailed). Regardless of the target type, we found that shorter contact durations led to higher post-impact kinetic energies. While strikes against the stiff material had shorter contact duration than those against the compliant material, a transition point occurred at a 5 ms contact duration, such that strikes with shorter contact durations, regardless of material, were able to impart much more energy than impacts with longer contact durations. Once the contact duration exceeded 7 ms, the energetic exchange of all of the impacts shared a similar, low output.

We used statistical models to compare the effects of multiple parameters on the amount of post-impact kinetic energy. The multilevel model was more predictive than the linear regression model (Akaike weight of 0.79 versus 0.21); therefore, we report the

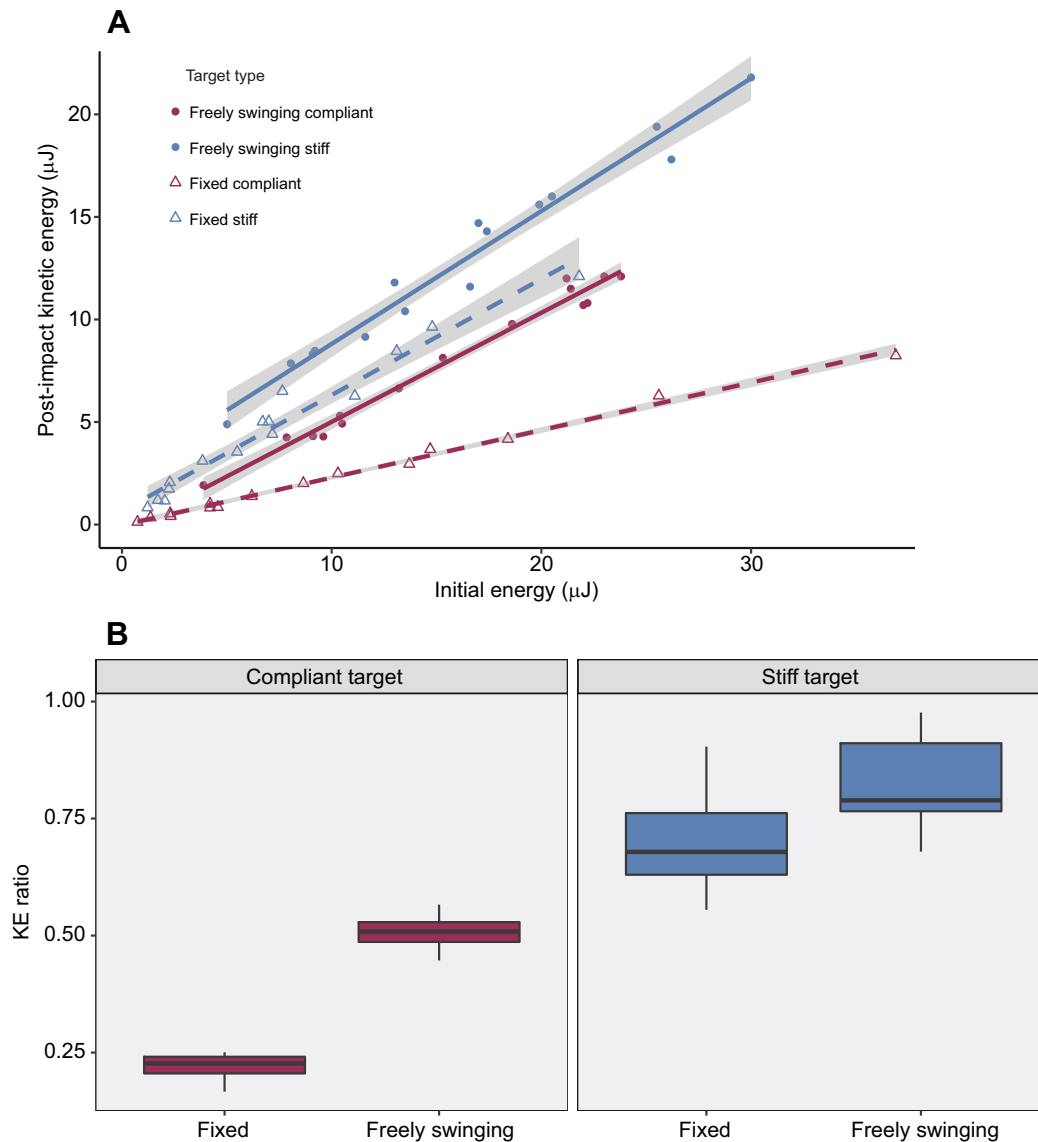


Fig. 4. Validation tests confirm the mICP's ability to consistently resolve and distinguish among target configurations across varying initial energy settings. (A) Across all target types, increasing the initial energy delivered by the validation impactor leads to a consistent increase in post-impact kinetic energy. Each point represents the measurements from a single test. (B) As indicated by the higher kinetic energy (KE) ratios, more energy is transferred for impacts against freely swinging targets than against fixed targets and for impacts against a stiff target than a compliant target.

statistical findings from the multilevel model. Changing the target material from compliant to stiff increased the post-impact kinetic energy more than changing the target from freely swinging to fixed (target material intercept: 2.76; target condition intercept: 1.45). Decreasing contact duration had the strongest effect on post-impact kinetic energy (intercept: -2.77), when compared with the other parameters (distance: -0.01 , ant: -0.34 , sequence: -0.20). Intercepts for each ant are presented in Fig. S2. See Figs S1 and S2 for the outputs of the multilevel model.

DISCUSSION

We measured sub-millisecond, microJoule impacts from trap-jaw ant strikes against targets with different masses and material properties through the use of the mICP. We discovered that the impact energetics of trap-jaw strikes are most strongly affected by material compliance, such that post-impact kinetic energy was nearly three times larger for stiff targets than compliant targets. By contrast, whether or not the target pendulum was fixed or freely swinging had relatively little

effect on energetic exchange. When the target was freely swinging, the ant's pendulum consistently recaptured the majority of the impact's energy. Contact duration – the duration from initial impact to final separation of the mandibles from the target – was a key influence on energy transfer, with shorter contact durations correlating with higher post-impact kinetic energy. These findings establish that impacts, even at these tiny scales, are influenced by target material properties, and that these features of energetic exchange are likely central to the diverse uses of trap-jaw strikes, as we discuss below. Our validation of the accuracy and consistency of the mICP sets the stage for future studies that measure the energetics of transient impacts against diverse targets and opens up the potential to reveal the principles of high acceleration impacts in tiny systems.

Impact energetics of varying target materials

Target material influenced the impact energetics of trap-jaw strikes. Maximum post-impact energy was measured in strikes against stiff targets (Fig. 6) with 5% of these strikes (6/116 strikes) within 5 μJ of

Table 1. Kinetic energy ratio and statistical results for tests where the energy source was the validation impactor

	Fixed target pendulum		Freely swinging target pendulum	
	Compliant	Stiff	Compliant	Stiff
Kinetic energy ratio mean \pm s.d.	0.22 \pm 0.03	0.69 \pm 0.11	0.51 \pm 0.03	0.82 \pm 0.10
<i>F</i> -test <i>k</i> -value ($k_{critical}=1.39$)	0.36	1.41*	0.43	1.29
Number of tests	15	15	15	15

During the micro impact characterization pendulum (mICP) validation tests, more impact energy is converted to kinetic energy for impacts against stiff targets than against compliant targets and against freely swinging targets than against fixed targets.

The kinetic energy (KE) ratio is the post-impact kinetic energy divided by the initial energy. The KE ratio for each target type is the mean of the KE ratios calculated for all 15 tests. To test how consistently the pendulum device performs across target types, the standard deviation of the KE ratio for each target type is compared with the group standard deviation of KE ratio through an *F*-test. The asterisk indicates that the standard deviation of the KE ratio is statistically higher for fixed stiff targets than all other target types.

the average maximum kinetic energy of unobstructed trap-jaw strikes (48 μ J for both mandibles; Sutton et al., in review). A previous study measured the kinetic energy of trap-jaw ants striking and jumping off of a hard-plastic substrate (10 μ J jump kinetic energy; Patek et al., 2006), which was stiffer than our compliant target (Sorbothane), but not as stiff as our stiff target (spring steel). Congruent with these material properties, the kinetic energy of these freely jumping ants was higher than the post-impact kinetic energy of the ant pendulum measured for the fixed, compliant Sorbothane target (6 μ J) and lower than strikes against the stiff spring steel target (21 μ J; Fig. 6).

With our findings, we can perform a back-of-the-envelope comparison to ask whether impacts performed at the spatial and temporal scale of the ant's strike differ from the scaled-up standard drop tests performed on these same materials (28 g weight dropped from height of 400 mm; ASTM International, 2019b). Trap jaw ant mandibles impact the target with an acceleration that is four orders of magnitude higher than the acceleration of the drop test weight (ASTM International, 2019b). The drop tests exhibit 4% energy return (post-impact energy/input energy) with 30 Durometer Sorbothane and 11% for the harder 50 Durometer Sorbothane (Sorbothane, 2018). Assuming a 48 μ J mandible strike input (Sutton et al., in review), trap-jaw ant strikes exhibit 12% energy return with the 40 Durometer Sorbothane used in our fixed target

experiments. Therefore, the impact energetics of a trap-jaw strike result in a higher energy return than in a drop test against a far harder material. The extraordinary acceleration of trap jaw mandibles may subject the target materials to high strain rates, which cause the material to behave as if it were more stiff material (Karunaratne et al., 2018). This comparison supports the need for performing impact tests, especially for such high acceleration impacts, at the appropriate biological scale and behavior of the organisms.

Impact energetics of fixed versus freely swinging targets

Our experiments comparing energy exchange against a fixed and freely swinging target reveal the role of target mass in energy exchange. During impact with a fixed or high inertia target, the amount of target puncture and deformation should be greater than in a freely swinging target. The mICP measures the energy transformed into motion of the target and impactor, collectively known as the post-impact kinetic energy. The post-impact kinetic energy of strikes against a freely swinging 0.4 g target was similar to the post-impact kinetic energy of strikes against a fixed target. This trend held for both target materials tested and suggests that with regards to energy transformed into motion for strikes of this scale, a 0.4 g target behaves similarly to a restrained target and that additional energy losses are similar in both.

This finding has implications for the threshold mass of trap-jaw ant targets in the wild that respond effectively like fixed targets. Other than the ground during mandible jumps, natural targets are rarely fixed in place. However, objects that are much heavier than the ant, such as large organisms or rocks, are effectively fixed in place because of their inertia. While more tests are needed to assess the effect of target shape and material, for flat targets with a mass of 0.4 g or greater, the trap-jaw ants are effectively striking a fixed target. This is similar in principle to puncture systems: for example, when a viper fang is driven into compliant, freely moving blocks of increasing mass, increasing target mass increases puncture depth until a critical target mass at which puncture depth no longer increases (Anderson et al., 2019). In our experiments and these puncture experiments, increasing the mass of the target past a certain critical mass did not have an effect on the measured form of energy exchange.

Impacts against a freely swinging target reveal the substantial inelasticity of impacts at these scales. Assuming a perfectly elastic collision with conservation of momentum, we expect the ant, which is roughly 1/60th of the target mass, to have a post-impact velocity 60 times greater than that of the target. However, the kinetic energy of the ant pendulum was only 1.53 times and 1.65

Table 2. Live trap-jaw ant impact energetics, contact duration and sample sizes during strikes against fixed and freely-swinging pendulums outfitted with either compliant or stiff targets

	Fixed target pendulum		Freely swinging target pendulum	
	Compliant	Stiff	Compliant	Stiff
Post-impact kinetic energy (μ J)				
Overall (mean \pm s.d.)	6.5 \pm 4.8	21.5 \pm 11.9	6.4 \pm 4.4	21.0 \pm 11.5
Ant pendulum (range)	1.1–21.9	5.5–59.5	0.8–13.2	2.6–31.4
Target pendulum (range)	NA	NA	0.6–10.3	1.6–25.7
Energy from each pendulum (μ J)				
Ant pendulum (mean \pm s.d.)	6.5 \pm 4.8	21.5 \pm 11.9	4.1 \pm 2.6	12.6 \pm 6.8
Target pendulum (mean \pm s.d.)	NA	NA	2.6 \pm 1.8	8.4 \pm 4.8
Ant pendulum energy:target pendulum energy	NA	NA	1.65	1.53
Contact duration (ms; mean \pm s.d.)	7.9 \pm 0.0022	4.5 \pm 0.0015	6.2 \pm 0.0007	3.9 \pm 0.0008
Sample size (19 ants, 3–23 strikes per ant)	50	52	55	55

The fixed target pendulum does not move. Therefore, no kinetic energy from the target is reported for those tests (indicated with NA) and the overall post-impact kinetic energy and ant pendulum energy are identical, because only the ant pendulum is moving.

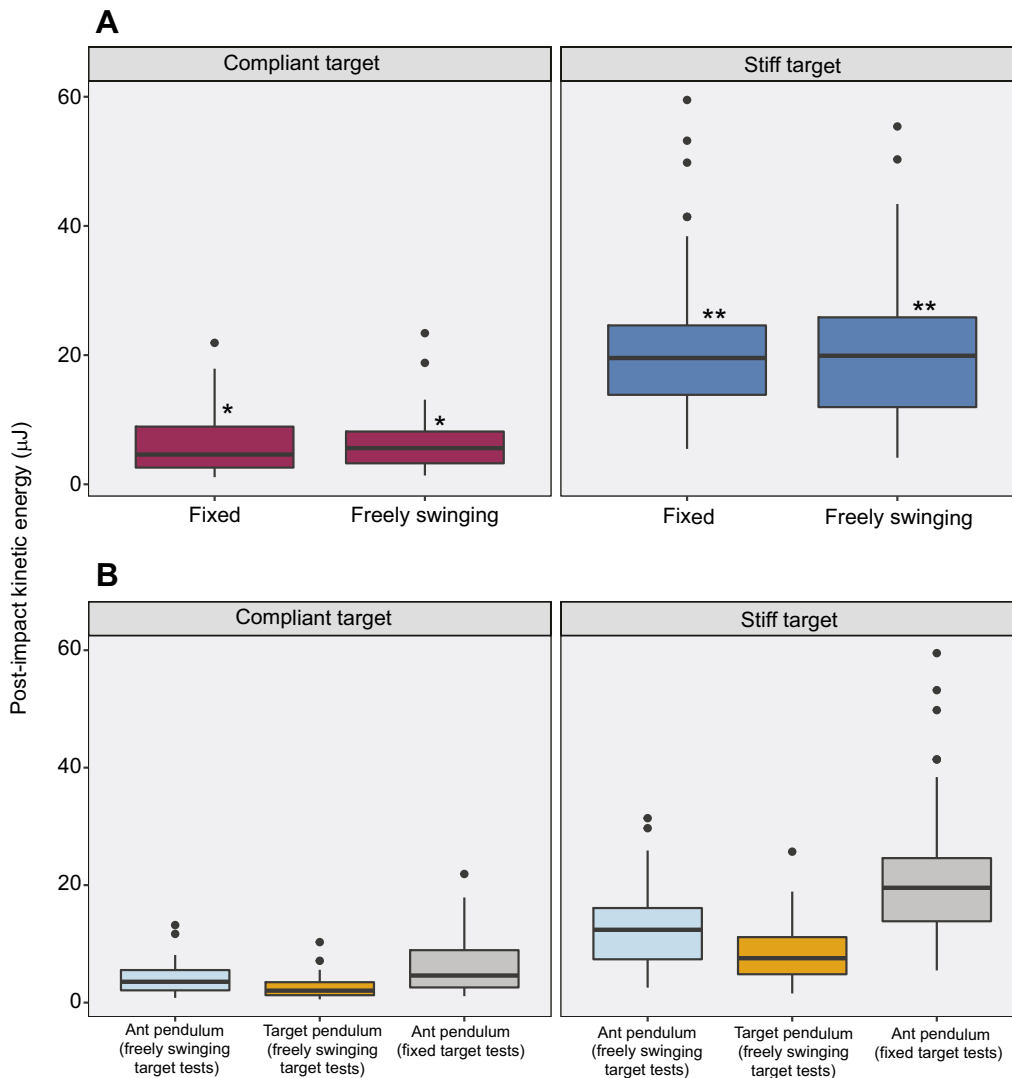


Fig. 5. Tests with trap-jaw ants as the energy source reveal that more energy is transferred during impacts against a stiff target than against a compliant target while the distribution of energy into the ant and target are similar. (A) With a live trap-jaw ant as the energy source, target material has a greater effect than target condition (free versus fixed target pendulum) on post-impact kinetic energy. Statistically significant differences are indicated when the number of asterisks above each bar differ. (B) For freely swinging targets, more post-impact kinetic energy is measured in the ant pendulum (light blue) than in the target pendulum (orange). The post-impact kinetic energy for fixed targets is determined solely by motion in the ant pendulum (gray).

times greater than the target pendulum for stiff targets and compliant targets, respectively (Fig. 5B). This discrepancy from idealized elastic collisions likely arises from the substantial inelasticity of the impacts.

One final area worthy of more investigation is the measurement of the actual energetic input of the ant strike during the mICP tests. Given current technology, the mandibles move during seven frames or less prior to impacting the target ($300,000 \text{ frames s}^{-1}$). Future experiments could incorporate calibration targets to account for friction and additional instrumentation to directly measure deformation and heat energy. Particles embedded in target materials could be tracked during impact to estimate how much impact energy is converted to deformation (Anderson et al., 2019).

Contact duration on impact energetics

Contact duration emerged as a key variable explaining impact energetics, and is particularly relevant for systems with rotational impacts such as the trap-jaw ant mandibles. Unlike classic examples of spring-loaded carts in which a spring is in contact with the other cart prior to energy release, the trap-jaw ant mandibles must be positioned away from the target to allow space for rotation and impact. In fact, live ants carefully position themselves at a set distance from their targets prior to firing their jaws. This distance is thought to be mediated by 0.6 to 1.2 mm-long trigger hairs which protrude out from the mandibles at an angle (Gronenberg and Tautz, 1994). These hairs are often associated with stimulating the release of the mandible strike (Just and Gronenberg, 1999). In our mICP tests, the ant

Table 3. Targets made from the same material did not have significantly different median post-impact kinetic energy

Post-impact kinetic energy compared (target 1–target 2)	Median (μJ) (target 1, target 2)	Sample size (no. strikes) (target 1, target 2)	W-value	P
Fixed compliant–free compliant	4.61×10^{-6} , 5.60×10^{-6}	50, 55	1352.5	0.8877
Fixed stiff–free stiff	1.96×10^{-5} , 1.99×10^{-5}	52, 55	1447	0.9181
Fixed compliant–fixed stiff	4.61×10^{-6} , 1.96×10^{-5}	50, 52	185.5	$\ll 0.001$
Fixed compliant–free stiff	4.61×10^{-6} , 1.99×10^{-5}	50, 55	265	$\ll 0.001$
Free compliant–free stiff	5.60×10^{-6} , 1.99×10^{-5}	55, 55	251.5	$\ll 0.001$
Free compliant–fixed stiff	5.60×10^{-6} , 1.96×10^{-5}	55, 52	174.5	$\ll 0.001$

Live trap-jaw ant statistics: two-tailed Mann–Whitney U-tests summary.

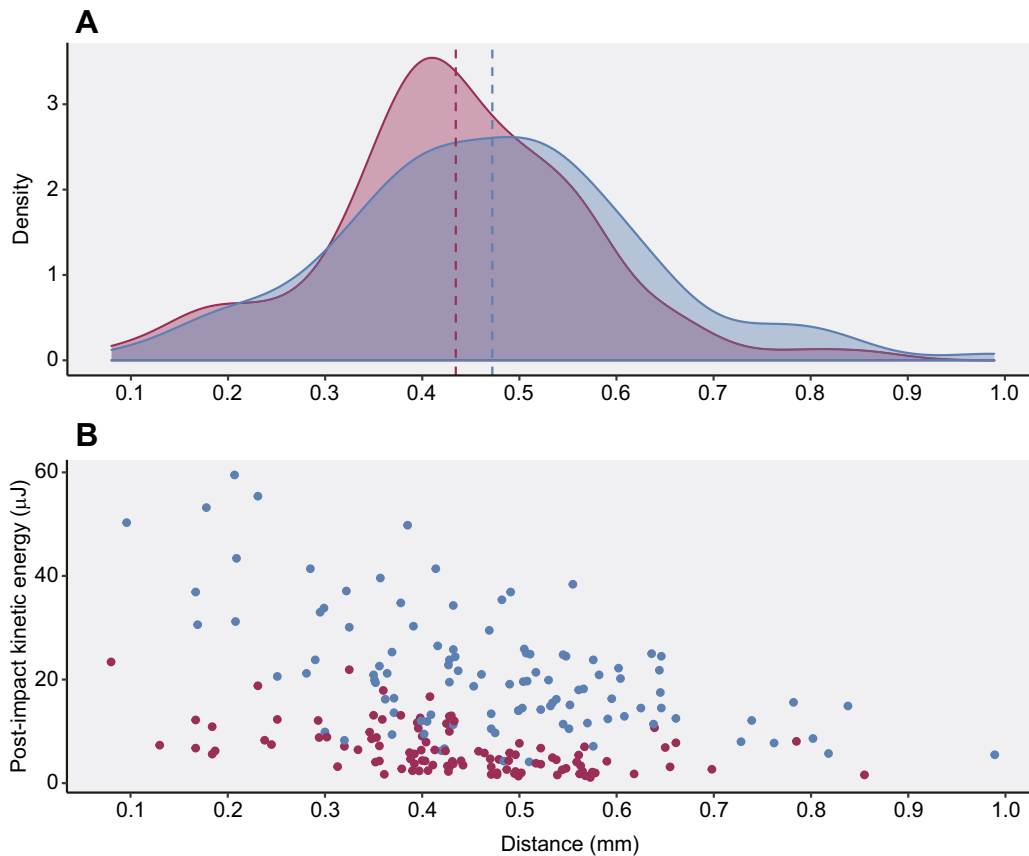


Fig. 6. Ants are positioned as consistently as possible relative to the target prior to each test and this target distance does not systematically influence post-impact kinetic energy. (A) The distributions of distance between ant mandibles and the target, in tests with compliant (maroon) and stiff (blue) materials, are centered close to 0.5 mm. Dashed vertical lines indicate the average distance between the ant and the target for strikes against the compliant and stiff targets. (B) The difference in post-impact kinetic energy between compliant (maroon) and stiff (blue) targets is larger than the effect of variation in distance between the ant and target.

mandibles were positioned approximately 0.5 mm away from the target before they were triggered. Regardless of material, shorter contact duration was correlated with higher post-impact kinetic energy. Target material appeared to limit contact duration and corresponding post-impact kinetic energy as evidenced by the overlap of post-impact kinetic energy for contact durations ranging from 4 to

6 ms (Fig. 7). Variation in contact duration is likely to be a consequence of target deformation, friction and damping (Cross, 2014), which is an interesting direction for future study. For example, future investigation into the effects of friction at these scales may reveal a range of biological tuning around this parameter, depending on the use of the impacting tool. This tuning may be manifested in the

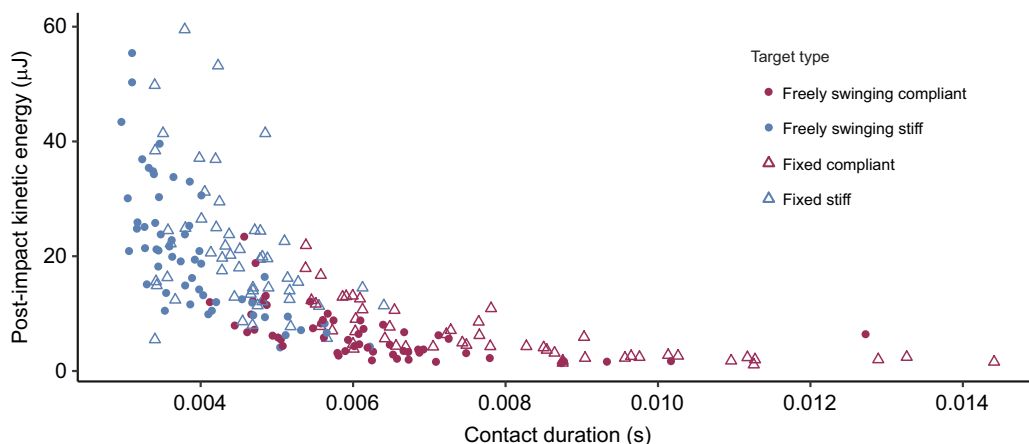


Fig. 7. In tests with trap-jaw ants as the energy source, decreasing contact duration of the mandibles with the target corresponds with higher post-impact kinetic energy. Fixed targets have higher post-impact kinetic energy for a given contact duration than freely swinging targets.

material composition of the tool and the microstructures on the tool, such as microstructures that increase friction or the presence of low friction regions along impacting surfaces.

Pendulum design and validation

Using a pendulum to accurately measure impact energetics at the scale of trap-jaw ant strikes requires either accounting for or mitigating the effects of friction and other non-conservative forces such as windage or vibrations. For materials tests, such as Charpy and Izod tests, vibrations are countered by using a large, sturdy pendulum arm. Friction and windage are addressed by running calibration tests to account for energy losses and by inspecting and swapping out bearings when needed (ASTM International, 2018b). However, our experiments tracked impact energetics that were orders of magnitude smaller than those measured in Charpy or Izod tests; therefore, we focused mICP design on reducing the error caused by these non-conservative forces. We reduced friction at the point of rotation by using air bearings that did not require lubrication between experiments, making the data acquired by this device consistent across trials. When addressing losses to vibrations, simply increasing pendulum size would reduce sensitivity to the small-scale impacts of the trap-jaw ant. Instead, we used a hollow carbon fiber rod.

The consistency and accuracy conferred by these design considerations were evident in the device testing and the trap-jaw ant experiments. Our validation tests revealed that increasing input energy did not lead to disproportionately larger losses. The device performed consistently across a range of energies relevant to the strikes of a trap-jaw ant and against different target types (Fig. 4). Additionally, if the mICP design resulted in substantial energetic losses, then the second pendulum should have doubled these losses and yielded even lower energy output. Instead, post-impact kinetic energy for strikes against free targets (i.e. with two pendulums) were similar to those against targets fixed in place (i.e. only one swinging pendulum).

Future applications of the mICP

We have thus far addressed how target material, target mass and contact duration affect impact dynamics with the trap-jaw ant as the energy source. We also established the mICP as an effective tool to measure small, transient impacts. In this final section, we consider how this device and this area of study can inform the biomechanics and ecology of transient impacts.

Natural target materials are composites with intricate shapes, materials and nanostructures that span the stiffnesses of the simple, monolithic materials tested in our study (Mayer and Sarikaya, 2002). By testing artificial targets of known stiffness or by mounting live organisms or tissue samples, the mICP can assess whether our findings are robust across a wider range of materials and structures. Biological targets offer opportunities to probe our initial findings on contact duration, specifically by performing controlled tests of target friction or internal damping, which may exhibit interactive effects with material stiffness. For example, impact tests against arthropod exoskeleton may reveal how viscoelastic materials respond to impact, including tuned impact energetic responses across different parts of animals, as has been found in the telson armor used during mantis shrimp ritualized fighting (Taylor and Patek, 2010; Taylor et al., 2019). Likewise, impact tests against loose media, such as sand or soil, may illuminate how impact-based jumps and strikes operate, while also providing a new spatio-temporal lens on the physics of particle jamming (Aguilar and Goldman, 2016; Huang et al., 2020; Umbanhowar and Goldman, 2010).

Relative target and impactor mass in small, transient impacts is key to how these mechanisms are used in nature, the effectiveness of using latch-mediated spring actuation (LaMSA), and how small-scale impacts could be used effectively in synthetic systems. LaMSA is only effective at small masses, specifically when spring recoil effectively accelerates a system (Ilton et al., 2018; Longo et al., 2019). Given that many LaMSA systems, such as trap-jaw ants, mantis shrimp and termites, are striking targets of widely varying mass, the dynamics of recoil and impact energetics, too, must vary. Our mICP allows systematic variation of target and impactor mass ratios to assess the effects of loading on impacts, and how this translates to effective use of these systems. In trap-jaw ants, there is a threshold above which the target is too massive to be pushed by the ant's spring-based mechanism and, likewise, because trap-jaw ants are not naturally fixed to the ground when striking, the ant's body may also act as a load that is pushed backwards by the strike. The mass of the target and even the ant's ability to anchor itself to the ground during a strike influence how the target mediates the outcome of the strike: whether the ant, target, or both will be launched away from the point of impact.

The challenge of studying natural systems, and a key tenet of ecomechanics, is to avoid alienating the behavior from its natural context while still being able to rigorously examine its biomechanics (Carrington Bell and Denny, 1994; Denny et al., 1985). Researchers have navigated this challenge by carefully monitoring or instrumenting organisms in their natural environment (Byrnes et al., 2008; Combes et al., 2010, 2012; Irschick et al., 2005) or isolating organisms or their parts in a controlled laboratory setting, then linking findings back to their natural behavior (Lentink et al., 2015; Melbourne et al., 2018; Spence et al., 2010). For both approaches, less disturbance to the organism makes drawing ecological conclusions from the data easier. This challenge is made more difficult when studying small organisms and complex behaviors such as impact, both common in LaMSA. We envision the mICP as an effective tool for rigorously studying ultrafast impacts (Larabee and Suarez, 2014; Larabee et al., 2018; Seid et al., 2008; Wood et al., 2016) and jumps (with kinematics that may be tuned through impact dynamics; Bonduriansky, 2002; Brackenbury and Hunt, 1993; Burrows, 2003; Farley et al., 2019) against targets that are representative of their equally diverse ecology. As long as an organism can be mounted to the impactor pendulum and encouraged to strike the target, the mICP is capable of testing a range of energy sources against synthetic or live targets. Hopefully, our intriguing results from trap-jaw ant impacts debuting the capabilities of our mICP will encourage new discoveries at the challenging and fascinating scales of high acceleration, small mass impacts in biology and synthetic systems.

APPENDIX

Using the mICP as a calibrated initial impact energy measurement tool

We designed and applied the mICP in the main study to measure energy exchange across different targets; however, the mICP could be also used to calculate the actual energetic input of an impacting organism. In this section, we explain how the mICP could be used as a calibrated tool to measure the initial energy of impact and provide an example from our trap-jaw ant experiments. In order to use the mICP to calculate the initial impact energy delivered by a live organism, key assumptions must be made about the similarities between impactor calibration tests (when the impactor pendulum is raised to a known height, and therefore, the input potential energy is known) and the energy delivery method by the organism (when the impactor has the organism attached to it as the energy source).

If one assumes that the KE ratios from the impactor tests are equivalent to calculations of the coefficients of restitution between the impacting organism and its target, then it is also necessary to assume that the interaction between the impactor and the target is the same in both the calibration tests and in the tests with a live animal as the energy source. In other words, calibration of the impactor must be carefully designed to adequately represent the interaction between the organism and the target. Along with matching the materials interacting in both tests, impact velocity and method of impact should match. Thus, the validity of the KE ratio as the coefficient of restitution depends on how the organism delivers energy and a similar impact delivery mechanism in the calibration tests. This issue obviously varies depending on which study organisms are mounted to the mICP.

We tested this approach using our trap-jaw ant impact dataset presented in the main text. We found that mean strike energy is fairly consistent across targets and falls within the known outputs of trap-jaw ants. However, owing to differences between energy delivery in our validation impactor tests and energy delivery by a trap-jaw ant, some challenges in interpreting the data arise. To calculate the initial energy delivered by the trap-jaw ants for each target type, we divided the post-impact kinetic energy by the average kinetic energy ratio for each target type that we measured from our calibration tests with a raised impactor. We expected that the initial energy from the ants would be consistent across target types, assuming that trap-jaw ants do not adjust the amount of energy delivered from their strikes depending on the target.

We found that the average amount of energy delivered by the ants as determined by this method was similar for all targets except for the freely swinging compliant target (Fig. S3, Table S1). Additionally, several measurements exceeded the energy estimations based on another study of unconstrained strikes (Sutton et al., in review). These exceptionally high energy values and the significantly different energy measurements for strikes against freely swinging compliant targets suggest that the assumption of similar impact dynamics with a validation impactor and live ant is not valid. Our impactor delivered energy by swinging into the target while the trap-jaw ant delivers energy by rotating two mandibles against a target. Even though we matched the ant mandible materials on our validation impactor by gluing ant mandibles to its surface, we still could not match the rotational impact dynamics of the live ant to fully match and calibrate the system. In sum, using the mICP as a calibrated system for accurately measuring input energy depends on the details of the particular system, and some systems, such as the rotational, transient impacts of trap-jaw ants, make this particularly challenging.

Acknowledgements

We thank Adrian Smith for the collection of the trap-jaw ants, and we greatly appreciate the Patek Lab, Phil Anderson and the Impulsive MURI team, especially Zeynep Temel, for their feedback and support. We would also like to acknowledge the Army Education Outreach Program and program mentors Chi-Yun Kuo and Alex Guo for their help in refining this project during its early stages.

Competing interests

The authors declare no competing or financial interests.

Author contributions

Conceptualization: J.F.J.; Methodology: J.F.J.; Validation: J.F.J., S.B., S.N.P.; Formal analysis: J.F.J., S.B., S.N.P.; Investigation: J.F.J.; Resources: S.N.P.; Writing - original draft: J.F.J.; Writing - review & editing: J.F.J., S.B., S.N.P.; Visualization: J.F.J.; Supervision: J.F.J., S.N.P.; Project administration: J.F.J., S.N.P.; Funding acquisition: S.N.P.

Funding

This material is based on work supported by the U.S. Army Research Laboratory and the U.S. Army Research Office under contract/grant number W911NF-15-1-0358.

Data availability

The R code used to analyze the data, the raw data tables and the computer-aided design files to 3D print the pendulum housings are available through the associated Dryad deposition (Jorge et al., 2021): <https://doi.org/10.5061/dryad.b2rbnzsmbm>.

Supplementary information

Supplementary information available online at <https://jeb.biologists.org/lookup/doi/10.1242/jeb.232157.supplemental>

References

- Aguiar, J. and Goldman, D. I.** (2016). Robophysical study of jumping dynamics on granular media. *Nature Phys.* **12**, 278–283. doi:10.1038/nphys3568
- Anderson, P. S. L.** (2018). Making a point: shared mechanics underlying the diversity of biological puncture. *J. Exp. Biol.* **221**, jeb187294. doi:10.1242/jeb.187294
- Anderson, P. S. L., LaCrosse, J. and Pankow, M.** (2016). Point of impact: the effect of size and speed on puncture mechanics. *Interface Focus* **6**, 20150111. doi:10.1098/rsfs.2015.0111
- Anderson, P. S. L., Crofts, S. B., Kim, J.-T. and Chamorro, L. P.** (2019). Taking a stab at quantifying the energetics of biological puncture. *Integr. Comp. Biol.* **59**, 1586–1596. doi:10.1093/icb/icz078
- ASTM International** (2018a). ASTM D256–10(2018), Standard Test Methods for Determining the Izod Pendulum Impact Resistance of Plastics. West Conshohocken, PA: D20 Committee.
- ASTM International** (2018b). ASTM D6110–18, Standard Test Method for Determining the Charpy Impact Resistance of Notched Specimens of Plastics. West Conshohocken, PA: D20 Committee.
- ASTM International** (2019a). E691–19 Practice for Conducting an Interlaboratory Study to Determine the Precision of a Test Method. West Conshohocken, PA: ASTM International.
- ASTM International** (2019b). D2632–15(2019) Standard Test Method for Rubber Property—Resilience by Vertical Rebound. West Conshohocken, PA: ASTM International.
- Biewener, A. A. and Patek, S. N.** (2018). *Animal Locomotion*, 2nd edn. Oxford: Oxford University Press.
- Bonduriansky, R.** (2002). Leaping behaviour and responses to moisture and sound in larvae of piophilid carrion flies. *Can. Entomol.* **134**, 647–656. doi:10.4039/Ent134647-5
- Brackenbury, J. and Hunt, H.** (1993). Jumping in springtails: mechanism and dynamics. *J. Zool.* **229**, 217–236. doi:10.1111/j.1469-7998.1993.tb02632.x
- Burrows, M.** (2003). Froghopper insects leap to new heights. *Nature* **424**, 509–509. doi:10.1038/424509a
- Byrnes, G., Lim, N. T.-L. and Spence, A. J.** (2008). Take-off and landing kinetics of a free-ranging gliding mammal, the Malayan colugo (*Galeopterus variegatus*). *Proc. R. Soc. B* **275**, 1007–1013. doi:10.1098/rspb.2007.1684
- Carlin, N. F. and Gladstein, D. S.** (1989). The “bouncer” defense of *Odontomachus ruginodis* and other *Odontomachus* ants (Hymenoptera: Formicidae). *Psyche* **96**, 1–19. doi:10.1155/1989/96595
- Carrington Bell, E. and Denny, M. W.** (1994). Quantifying “wave exposure”: a simple device for recording maximum velocity and results of its use at several field sites. *J. Exp. Mar. Biol. Ecol.* **181**, 9–29. doi:10.1016/0022-0981(94)90101-5
- Combes, S. A., Crall, J. D. and Mukherjee, S.** (2010). Dynamics of animal movement in an ecological context: dragonfly wing damage reduces flight performance and predation success. *Biol. Lett.* **6**, 426–429. doi:10.1098/rsbl.2009.0915
- Combes, S. A., Rundle, D. E., Iwasaki, J. M. and Crall, J. D.** (2012). Linking biomechanics and ecology through predator-prey interactions: flight performance of dragonflies and their prey. *J. Exp. Biol.* **215**, 903–913. doi:10.1242/jeb.059394
- Cross, R.** (2014). Impact of sports balls with striking implements. *Sports Eng* **17**, 3–22. doi:10.1007/s12283-013-0132-0
- Denny, M. W., Daniel, T. L. and Koehl, M. A. R.** (1985). Mechanical limits to size in wave-swept organisms. *Ecol. Monogr.* **55**, 69–102. doi:10.2307/1942526
- Farley, G. M., Wise, M. J., Harrison, J. S., Sutton, G. P., Kuo, C. and Patek, S. N.** (2019). Adhesive latching and legless leaping in small, worm-like insect larvae. *J. Exp. Biol.* **222**, jeb201129. doi:10.1242/jeb.201129
- Gibson, J. C., Larabee, F. J., Touchard, A., Orivel, J. and Suarez, A. V.** (2018). Mandible strike kinematics of the trap-jaw ant genus *Anochetus* Mayr (Hymenoptera: Formicidae). *J. Zool.* **306**, 119–128. doi:10.1111/jzo.12580
- Gronenberg, W.** (1995). The fast mandible strike in the trap-jaw ant *Odontomachus*: I. Temporal properties and morphological characteristics. *J. Comp. Physiol. A* **176**, 391–398. doi:10.1007/BF00219064
- Gronenberg, W. and Tautz, J.** (1994). The sensory basis for the trap-jaw mechanism in the ant *Odontomachus bauri*. *J. Comp. Physiol. A* **174**, 49–60. doi:10.1007/BF00192005
- Hao, W., Yao, G., Zhang, X. and Zhang, D.** (2018). Kinematics and mechanics analysis of trap-jaw ant *Odontomachus monticola*. *J. Phys. Conf. Ser.* **986**, 012029. doi:10.1088/1742-6596/986/1/012029

- Hedrick, T. L. (2008). Software techniques for two- and three-dimensional kinematic measurements of biological and biomimetic systems. *Bioinspir. Biomim.* **3**, 034001. doi:10.1088/1748-3182/3/3/034001
- Huang, K., Hernández-Delfin, D., Rech, F., Dichtl, V. and Hidalgo, R. C. (2020). The role of initial speed in projectile impacts into light granular media. *Sci. Rep.* **10**, 3207. doi:10.1038/s41598-020-59950-z
- Ilton, M., Bhamla, M. S., Ma, X., Cox, S. M., Fitchett, L. L., Kim, Y., Koh, J., Krishnamurthy, D., Kuo, C.-Y., Temel, F. Z. et al. (2018). The principles of cascading power limits in small, fast biological and engineered systems. *Science* **360**, eaao1082. doi:10.1126/science.aao1082
- Ilton, M., Cox, S. M., Egelmeers, T., Sutton, G. P., Patek, S. N., Crosby, A. J. (2019). The effect of size-scale on the kinematics of elastic energy release. *Soft Mat.* **15**, 9579-9586. doi:10.1039/C9SM00870E
- Irschick, D. J., Herrel, A., Vanhooydonck, B., Huyghe, K. and van Damme, R. (2005). Locomotor compensation creates a mismatch between laboratory and field estimates of escape speed in lizards: a cautionary tale for performance-to-fitness studies. *Evolution* **59**, 1579-1587. doi:10.1111/j.0014-3820.2005.tb01807.x
- Jayaram, K., Mongeau, J.-M., Mohapatra, A., Birkmeyer, P., Fearing, R. S. and Full, R. J. (2018). Transition by head-on collision: mechanically mediated manoeuvres in cockroaches and small robots. *J. R. Soc. Interface* **15**, 20170664. doi:10.1098/rsif.2017.0664
- Just, S. and Gronenberg, W. (1999). The control of mandible movements in the ant *Odontomachus*. *J. Insect Physiol.* **45**, 231-240. doi:10.1016/S0022-1910(98)00118-8
- Jorge, J., Bergbreiter, S. and Patek, S. (2021). Data for: Pendulum-based measurements reveal impact dynamics at the scale of a trap-jaw ant. Dryad, Dataset, <https://doi.org/10.5061/dryad.b2rbnzsbm>
- Karunaratne, A., Li, S. and Bull, A. M. J. (2018). Nano-scale mechanisms explain the stiffening and strengthening of ligament tissue with increasing strain rate. *Sci. Rep.* **8**, 3707. doi:10.1038/s41598-018-21786-z
- Larabee, F. J. and Suarez, A. V. (2014). The evolution and functional morphology of trap-jaw ants (Hymenoptera: Formicidae). *Myrmecological News* **20**, 25-36.
- Larabee, F. J. and Suarez, A. V. (2015). Mandible-powered escape jumps in trap-jaw ants increase survival rates during predator-prey encounters. *PLoS ONE* **10**, e0124871. doi:10.1371/journal.pone.0124871
- Larabee, F. J., Gronenberg, W. and Suarez, A. V. (2017). Performance, morphology and control of power-amplified mandibles in the trap-jaw ant *Myrmoteras* (Hymenoptera: Formicidae). *J. Exp. Biol.* **220**, 3062-3071. doi:10.1242/jeb.156513
- Larabee, F. J., Smith, A. A. and Suarez, A. V. (2018). Snap-jaw morphology is specialized for high-speed power amplification in the Dracula ant, *Mystrum camillae*. *R. Soc. Open Sci.* **5**, 181447. doi:10.1098/rsos.181447
- Lee, S., Novitskaya, E. E., Reynante, B., Vasquez, J., Urbaniak, R., Takahashi, T., Woolley, E., Tombolato, L., Chen, P.-Y. and McKittrick, J. (2011). Impact testing of structural biological materials. *Mater. Sci. Eng. C* **31**, 730-739. doi:10.1016/j.msec.2010.10.017
- Lentink, D., Haselsteiner, A. F. and Ingersoll, R. (2015). *In vivo* recording of aerodynamic force with an aerodynamic force platform: from drones to birds. *J. R. Soc. Interface* **12**, 20141283. doi:10.1098/rsif.2014.1283
- Longo, S. J., Cox, S. M., Azizi, E., Ilton, M., Olberding, J. P., St Pierre, R. and Patek, S. N. (2019). Beyond power amplification: latch-mediated spring actuation is an emerging framework for the study of diverse elastic systems. *J. Exp. Biol.* **222**, jeb197889. doi:10.1242/jeb.197889
- Mayer, G. and Sarikaya, M. (2002). Rigid biological composite materials: structural examples for biomimetic design. *Exp. Mech.* **42**, 395-403. doi:10.1007/BF02412144
- McElreath, R. (2016). *Statistical Rethinking: a Bayesian Course with Examples in R and Stan*. Boca Raton: CRC Press/Taylor & Francis Group.
- McHenry, M. J., Anderson, P. S. L., Van Wassenbergh, S., Matthews, D. G., Summers, A. P. and Patek, S. N. (2016). The comparative hydrodynamics of rapid rotation by predatory appendages. *J. Exp. Biol.* **219**, 3399-3411. doi:10.1242/jeb.140590
- Melbourne, L. A., Denny, M. W., Harniman, R. L., Rayfield, E. J. and Schmidt, D. N. (2018). The importance of wave exposure on the structural integrity of rhodoliths. *J. Exp. Mar. Biol. Ecol.* **503**, 109-119. doi:10.1016/j.jembe.2017.11.007
- Patek, S. N., Baio, J. E., Fisher, B. L. and Suarez, A. V. (2006). Multifunctionality and mechanical origins: ballistic jaw propulsion in trap-jaw ants. *Proc. Natl Acad. Sci. USA* **103**, 12787-12792. doi:10.1073/pnas.0604290103
- Seid, M. A., Scheffrahn, R. H. and Niven, J. E. (2008). The rapid mandible strike of a termite soldier. *Curr. Biol.* **18**, R1049-R1050. doi:10.1016/j.cub.2008.09.033
- Spagna, J. C., Vakis, A. I., Schmidt, C. A., Patek, S. N., Zhang, X., Tsutsui, N. D. and Suarez, A. V. (2008). Phylogeny, scaling, and the generation of extreme forces in trap-jaw ants. *J. Exp. Biol.* **211**, 2358-2368. doi:10.1242/jeb.015263
- Spagna, J. C., Schelkopf, A., Carrillo, T. and Suarez, A. V. (2009). Evidence of behavioral co-option from context-dependent variation in mandible use in trap-jaw ants (*Odontomachus* spp.). *Naturwissenschaften* **96**, 243-250. doi:10.1007/s00114-008-0473-x
- Spence, A. J., Revzen, S., Seipel, J., Mullens, C. and Full, R. J. (2010). Insects running on elastic surfaces. *J. Exp. Biol.* **213**, 1907-1920. doi:10.1242/jeb.042515
- Swift, N. B., Hsiung, B.-K., Kennedy, E. B. and Tan, K.-T. (2016). Dynamic impact testing of hedgehog spines using a dual-arm crash pendulum. *J. Mech. Behav. Biomed. Mater.* **61**, 271-282. doi:10.1016/j.jmbbm.2016.03.019
- Taylor, J. R. A. and Patek, S. N. (2010). Ritualized fighting and biological armor: the impact mechanics of the mantis shrimp's telson. *J. Exp. Biol.* **213**, 3496-3504. doi:10.1242/jeb.047233
- Taylor, J. R. A., Scott, N. I. and Rouse, G. W. (2019). Evolution of mantis shrimp telson armour and its role in ritualized fighting. *J. R. Soc. Interface* **16**, 20190203. doi:10.1098/rsif.2019.0203
- Umbanhowar, P. and Goldman, D. I. (2010). Granular impact and the critical packing state. *Phys. Rev. E* **82**, 010301. doi:10.1103/PhysRevE.82.010301
- Vincent, J. F. V. and Wegst, U. G. K. (2004). Design and mechanical properties of insect cuticle. *Arthropod. Struct. Dev.* **33**, 187-199. doi:10.1016/j.asd.2004.05.006
- Wood, H. M., Parkinson, D. Y., Griswold, C. E., Gillespie, R. G. and Elias, D. O. (2016). Repeated evolution of power-amplified predatory strikes in trap-jaw spiders. *Curr. Biol.* **26**, 1057-1061. doi:10.1016/j.cub.2016.02.029